April 1981

Energy dependence of alignment in foil collision-excited *n*=3 states of He I

Timothy J. Gay
University of Nebraska - Lincoln, tgay1@unl.edu

H. G. Berry
Argonne National Laboratory, Argonne, Illinois

R. DeSerio
Argonne National Laboratory, Argonne, Illinois

H. P. Garnir
Argonne National Laboratory, Argonne, Illinois

R. M. Schectman
University of Toledo, Toledo, Ohio

See next page for additional authors

Phys. Rev. A 23, 1745 - 1760 (1981) [Issue 4 – April 1981]

Energy dependence of alignment in foil collision-excited n=3 states of He I

T. J. Gay [*,†,‡], H. G. Berry, R. DeSerio [*], and H. P. Garnir [§]
Physics Division, Argonne National Laboratory, Argonne, Illinois 60439

R. M. Schectman and N. Schaffel
Department of Physics and Astronomy, University of Toledo, Toledo, Ohio 43606

R. D. Hight [**] and D. J. Burns
Behlen Laboratory of Physics, The University of Nebraska, Lincoln, Nebraska 68588

Received 28 July 1980

We have measured the beam-foil collision-induced alignment of the $3p\ ^1P$, $3p\ ^3P$, $3d\ ^1D$, and $3d\ ^3D$ states of He I for He^+ beam energies between 30 and 1300 keV. The alignment of all four states is found to vary with beam-current density as well as energy. The number of secondary electrons emitted per incident ion, γ, has also been measured as a function of foil temperature and beam energy between 400 and 1400 keV. The rate of change of both alignment and γ with foil temperature exhibits a general correlation. The energy dependence of alignment may be understood in terms of simple impact-excitation collisions. We also discuss our results in terms of the Kupfer-Winter surface electric-field model. The interaction between atoms emerging from the foil and slow secondary electrons is considered.

URL: http://link.aps.org/abstract/PRA/v23/p1745

DOI: 10.1103/PhysRevA.23.1745

Energy dependence of alignment in foil collision-excited $n=3$ states of He I

T. J. Gay,*† H. G. Berry, R. DeSerio,* and H. P. Garnir§
Physics Division, Argonne National Laboratory, Argonne, Illinois 60439

R. M. Schectman and N. Schaffel
Department of Physics and Astronomy, University of Toledo, Toledo, Ohio 43606

R. D. Hight‖ and D. J. Burns
Behlen Laboratory of Physics, The University of Nebraska, Lincoln, Nebraska 68588

(Received 28 July 1980)

We have measured the beam-foil collision-induced alignment of the $3p\ ^1P$, $3p\ ^3P$, $3d\ ^1D$, and $3d\ ^3D$ states of He I for He^+ beam energies between 30 and 1300 keV. The alignment of all four states is found to vary with beam-current density as well as energy. The number of secondary electrons emitted per incident ion, γ, has also been measured as a function of foil temperature and beam energy between 400 and 1400 keV. The rate of change of both alignment and γ with foil temperature exhibits a general correlation. The energy dependence of alignment may be understood in terms of simple impact-excitation collisions. We also discuss our results in terms of the Kupfer-Winter surface electric-field model. The interaction between atoms emerging from the foil and slow secondary electrons is considered.

I. INTRODUCTION

With the advent of the beam-foil light source as a spectroscopic tool, considerable interest in the physics of the fast ion-foil-collision process has developed. Confirming the theoretical prediction of Macek,[1] Andrä[2] showed in 1970 that foil collision-excited states could be aligned, i.e., have a nonzero second moment of electron distribution. Such alignment manifests itself in the linear polarization of light emitted by the atoms downbeam from the foil. In 1974, Berry *et al.*[3] observed circularly polarized light when the foil was tilted about an axis perpendicular to the direction of the beam. Because the foil bulk is amorphous, this experiment demonstrated the essential surface character of the excitation process.[4] Considering that bound excited states of fast atoms or ions have an extremely short mean life in solids, this result is not surprising.[5]

Clearly, one step towards a comprehensive understanding of the beam-foil excitation and alignment process is the measurement of the energy dependence of alignment when the foil normal is parallel to the beam direction. To date, this has been done in three cases: Two groups[6-9] have determined the alignment of the $2P$ state in H between 10 and 2000 keV; in addition, our group has measured the alignment of the $3p\ ^1P$ and $4d\ ^1D$ states of He I between 20 and 1000 keV.[10,11] We found the alignment to depend not only on beam energy but beam-current density as well.[10] This latter effect was subsequently shown to result from the heating of the foil by the beam,[12] and we suggested that the observed alignment variations were caused by the change of secondary electron flux with foil temperature.

In this paper, we report measurements of the alignment of the $3p\ ^3P$, $3d\ ^1D$, and $3d\ ^3D$ states of He I between 25 and 1300 keV and further measurements of $3p\ ^1P$ alignment above 400 keV. These results thus provide a complete overview of the energy dependence of beam-perpendicular foil collision-induced alignment in the $n=3$ manifold of He I. The polarization temperature dependence[12] is seen to be a general feature of the data. We discuss the energy dependence results in terms of analogous single-collision data and the surface electric-field model of Kupfer and Winter,[8] and show that both hydrogen and helium results may be well understood in terms of simple ion-atom collisional interactions. In addition, we present measurements of secondary electron emission as a function of foil temperature for beam energies greater than 400 keV, thus extending the range of earlier measurements.[12] The dynamic interaction between He atoms emerging from the foil surface and these electrons is considered.

II. EXPERIMENT

A. Optical measurements

Measurements were made at four laboratories using four accelerators. He^+ beams above 400 keV were obtained from the Argonne Physics Division Dynamitron accelerator. All data between 225 and 400 keV were taken with the PN Van de Graaff at the University of Toledo. Measurements below 225 keV were made at Toledo and at the University of Chicago using a small electrostatic accelerator. Supplemental data taken with an electrostatic accelerator at the University of

Nebraska confirmed the Chicago and Toledo results for the $3p\,^3P$ and $3d\,^1D$ states between 75 and 375 keV.

The ion beam was collimated to a diameter of 4.8 mm upon entering the target chamber. Carbon foils between 5 and 6.5(± 1) $\mu g/cm^2$ were mounted on 1-mm thick Al foil holders having circular apertures 6.4 mm in diameter. Up to 23 of these holders could be mounted on a wheel and sequentially rotated into the beam. The beam was stopped in a Faraday cup. The target chambers at all four laboratories were pumped by metal oil diffusion pumps trapped by liquid nitrogen-chilled baffles. Nominal chamber pressures were 1×10^{-6} Torr or lower. Beam-energy calibrations were made by measuring the length of the slow $J,J'=2,1$ 659-MHz fine-structure beat in the He I $2s\,^3S$-$3p\,^3P$ 3889 Å transition. Calibration accuracy was better than 4% at all energies.

Photons emitted by foil-excited atoms were observed at 90° to the beam direction through a fused silica viewing port in the side of the chamber. For our case of cylindrically symmetric collision geometry in which the foil normal is parallel to the beam direction, the measured intensity of light polarized parallel or perpendicular to the beam may be written[13]

$$\begin{aligned} I_{\parallel}(t) &= C(t)[1+h^{(2)}G(t)A_0^{\mathrm{col}}(0)], \\ I_{\perp}(t) &= C(t)[1-\tfrac{1}{2}h^{(2)}G(t)A_0^{\mathrm{col}}(0)], \end{aligned} \tag{1}$$

where $C(t)$ contains the exponential decay factor and the oscillator strength of the transition, the angular acceptance and efficiency of the detector, and constants required to express I as a power flux. $G(t)$ describes the time-dependent transfer of alignment between orbital and spin (either nuclear or electronic) coordinates. In the case of ^{4}He and cylindrically symmetric excitation,

$$G(t)=\tfrac{1}{2}\sum_{J'J}\left(\frac{(2J+1)(2J'+1)}{(2S+1)}\begin{Bmatrix} J' & J & 2 \\ L & L & S \end{Bmatrix}^2\cos\omega_{J'J}t\right), \tag{2}$$

where J, J', L, and S are the quantum numbers of two fine-structure levels in the upper state. The cosine frequency corresponds to the respective fine-structure splitting. Equation (2) is derived assuming no collisional alignment of spins.[13-15] The term $h^{(2)}$ is given by[13]

$$h^{(2)}=(-1)^{L_i-L_f}\times\left(\begin{Bmatrix} L_i & L_i & 2 \\ 1 & 1 & L_f \end{Bmatrix}\Big/\begin{Bmatrix} L_i & L_i & 2 \\ 1 & 1 & L_i \end{Bmatrix}\right), \tag{3}$$

where i and f refer to the initial and final states in the transition.

$A_0^{\mathrm{col}}(0)$ is the Fano-Macek alignment parameter, and is the initial value of the second moment of electron distribution of the excited state along the beam axis. It may be written as a weighted average of the m_l population:

$$A_0^{\mathrm{col}}(0)=\frac{\sum_{m_l}[3m_l^2-l(l+1)]\sigma(m_l)}{l(l+1)\sum_{m_l}\sigma(m_l)}. \tag{4}$$

The quantities $G(t)$ and $h^{(2)}$ for the four $n=2$–3 He I transitions measured are

$(2s\,^1S-3p\,^1P,\ 5016\ \text{Å})$

$$G(t)=1,\quad h^{(2)}=-2, \tag{5}$$

$(2p\,^1P-3d\,^1D,\ 6678\ \text{Å})$

$$G(t)=1,\quad h^{(2)}=-1, \tag{6}$$

$(2s\,^3S-3p\,^3P,\ 3889\ \text{Å})$

$$G(t)=\tfrac{5}{18}(1+\tfrac{9}{5}\cos\omega_{21}t),\quad h^{(2)}=-2, \tag{7}$$

$(2p\,^3P-3d\,^3D,\ 5876\ \text{Å})$

$$G(t)=\tfrac{1}{150}(71+40\cos\omega_{32}t+35\cos\omega_{21}t),$$

$$h^{(2)}=-1. \tag{8}$$

The $J,J'=2,0$ and $1,0$ splittings in the $3p\,^3P$ level were spatially unresolved in our experiments and are not included in (7). The $3d\,^3D$ $J,J'=3,1$ beat was not observed due to its small amplitude and is neglected in (8).

Polarization measurements were made in one of two ways. In the first method, a film polarizer was rotated to measure relative values of $I_{\parallel}$ and $I_{\perp}$. In this manner, the polarization $P(t)$ may be determined:

$$P(t)=\frac{I_{\parallel}-I_{\perp}}{I_{\parallel}+2I_{\perp}}=\tfrac{1}{2}h^{(2)}G(t)A_0^{\mathrm{col}}(0). \tag{9}$$

This method has the disadvantage that one must carefully determine and correct for detector polarization bias. The other method used is described in detail by Berry *et al.*[16] The polarizing element (in this case a Glan-air prism polarizer) is fixed while a retarder plate is rotated. With this system, the linear polarization fraction (relative Stoke's parameter M/I) is most conveniently measured[16]

$$\begin{aligned} \frac{M}{I}&=\frac{I_{\parallel}-I_{\perp}}{I_{\parallel}+I_{\perp}}=\frac{2\eta}{(1-\cos\delta)-\eta(1+\cos\delta)}, \\ \eta&=\frac{I(\theta=n\pi/2)-I(\theta=(2n+1)\pi/4)}{I(\theta=n\pi/2)+I(\theta=(2n+1)\pi/4)}, \end{aligned} \tag{10}$$

where θ is the angle between the retarder's fast axis and the beam direction, δ is the retardance, and n is an integer.

In both cases, light from the beam was focused by a lens onto an image slit. Between the lens and the slit was mounted either a single rotatable film polarizer or a fixed Glan-air polarizer (nearest the slit) and a rotatable retardation plate. The film polarizer had a measured extinction coefficient of better than 1% over the wavelength range of our experiments. This system was used when count rates were low (high beam energies, singlet transitions) because a much larger image aperture could be employed with such a configuration. A 4-mm-diameter circular aperture, for example, was used to measure the singlet states above 500 keV. The Glan-air polarizer had a maximum acceptance angle of 9° and an effective circular aperture of 3 mm. The lens aperture in this optical configuration was 3.5 cm, while the nominal lens-slit distance was 30 cm (with variation from this depending on transition wavelength). Thus, light rays could make no larger than a 3° angle with the optic axis. The zero-order crystalline-quartz phase plate, manufactured by Karl Lambrecht, Inc., had a retardance angle δ measured to within 2° over the wavelength range of interest.

The light detection system consisted of a photomultiplier tube in a cooled housing masked by a 2.54-cm-diameter narrow-band interference filter. Polarization of light from the $2p\,^1P$–$3d\,^1D$ 6678 Å transition was measured using an ITT FW4034 S20 red sensitive tube cooled to dry ice temperature. All other transitions were measured using a Centronic 4249B tube cooled in a Peltier effect housing. Interference filters were obtained from the Oriel Corporation. They had peak transmission wavelengths (and full width at half-maximum bandwidths) of 3910 Å (110 Å), 5018 Å (12 Å), 5900 Å (100 Å), and 6700 Å (80 Å) for the 3889 Å, 5016 Å, 5876 Å, and 6678 Å transitions, respectively. These bandwidths were sufficiently narrow to exclude light from other helium transitions except the 6700 Å filter. Corrections for measurements made with this filter are discussed below.

Data acquisition was automated by an on-line minicomputer (Argonne) or microcomputer (Toledo, Chicago). Beam current registered at the Faraday cup was digitized and photons were counted for a present number of digitizer counts. Counting time was monitored, enabling the computer to subtract background or dark counts automatically. Data were taken in one of four ways, depending on the optical train in use and whether a singlet or triplet state was being measured.[17]

(a) Singlet states, rotating polarizer. Polarization as a function of distance from the foil was checked for constancy to insure that cascading and spurious reflected light were not affecting the data. The polarization P was then measured at a fixed position down beam, typically 3–4 mm from the foil.

(b) Singlet states, rotating phase plate. The parameter η (and thereby M/I) was checked for constancy downbeam from the foil and then measured at a fixed position.

(c) Triplet states, rotating polarizer. The polarization $P(t)$ was measured as a function of distance from the foil. $A_0^{\rm col}$ (0) was extracted either by fitting the results to the cosinusoidal form of (7) or (8) and (9) or by simply averaging $P(t)$ over an integral number of beat wavelengths. The first beat was not included in the analysis to avoid possible problems caused by light reflected from the foil or foil holder. In the ^3D case, where it was not practical to move the foil the length of the slow 76-MHz (ω_{32}) beat, the second and third 1325-MHz (ω_{21}) beats were averaged and appropriate corrections made for the slow beat. Equation (9) must be corrected for finite detector resolution when the cosine fitting procedure is used. This resolution was determined by attaching a Hg light source collimated to 0.05 mm to the foil wheel and moving it on the beam axis past the optical train. Agreement between the two methods of data analysis was always considerably better than statistical uncertainty in the measurements.

(d) Triplet states, rotating phase plate. Measuring $M/I(t)$ instead of $P(t)$ complicates the analysis somewhat. The linear polarization of the 3889-Å transition, is given by

$$M/I(t)=\frac{-\frac{5}{6}(1+\frac{9}{5}\cos\omega_{21}t)A_0^{\rm col}(0)}{2-\frac{5}{18}(1+\frac{9}{5}\cos\omega_{21}t)A_0^{\rm col}(0)}\ . \tag{11}$$

The equivalent expression for the ^3D transition is

$$M/I(t)=\frac{-\frac{1}{100}(71+40\cos\omega_{32}t+35\cos\omega_{21}t)A_0^{\rm col}(0)}{2-\frac{1}{300}(71+40\cos\omega_{32}t+35\cos\omega_{21}t)A_0^{\rm col}(0)}\ . \tag{12}$$

The triplet alignment parameters were obtained using these formulas. Corrections to account for finite detector resolution in, e.g., (11) and (12) were negligible.

In general, we attempted to obtain absolute statistical uncertainties in the measured asymmetries (P or η) of less than 0.5%. This corresponded to accumulating between 30 000 and 150 000 counts for a given polarizer or phase plate position over the course of the run. The phase plate and film polaroid were rotated through 360° to eliminate the effects of possible asymmetries in these elements. Typically 20 to 40 revolutions

would be made for a complete measurement. Counting rates were highly variable, depending on chamber geometry, optical train, beam energy, and atomic transition. Rates as high as 3000 counts per second were measured at low energy for the 3889-Å transition using a 0.5-mm-wide slit. At 1.2 MeV, using a 4-mm-diameter circular image aperture, 5016-Å counting rates with a 5-μA beam were 20 /sec, including a dark count of 5 /sec. Single measurements took between 10 min and 2 h. Photomultiplier dark counts were typically 3–10/sec and were unpolarized. This signal was the same with and without beam except for the 3889-Å light for which there was a small current dependent background, presumably due to neutralization and excitation of the He^+ beam by residual gas in the chamber. This background signal was about 1% of the signal with the foil in place and was only marginally polarized. Its contribution was included in the analysis.

Statistical errors in $A_0^{col}(0)$ are typically between 0.5 and 0.8% and never larger than 0.9%. The determination of the phase delay, δ, is good to 2° at all wavelengths. This corresponds to a maximum fractional error [see (10)] of 4% in A_0^{col} for the 6678 Å $3p\,^1P$–$3d\,^1D$ transition, where $\delta = 86° \pm 2°$. For the 3889-Å $2s\,^3S$–$3p\,^3P$ transition, where $\delta = 156° \pm 2°$, the fractional uncertainty is about 1% of $A_0^{col}(0)$. When the rotating polarizer system was used, instrumental polarization was measured by focusing the system on an unpolarized light source (e.g., incandescent light diffused through a colloidal suspension) and determining the apparent asymmetry. Instrumental polarization, P, was always less than 0.2%, with the statistical error of the determination typically being 0.2 to 0.3%. Alignment values were corrected for instrumental polarization where appropriate, with the additional statistical error included. Instrumental depolarization effects due to residual birefringence of the fused silica chamber window and collection lens were determined (by rotation of these elements) to be negligible.

As a consistency check, polarizations for all four transitions were measured at 100, 200, and 500 keV using both optical systems. The values agreed within statistical error, and no systematic effects were observed. As a result, errors due to instrumental polarization and phase delay uncertainty may be considered to be minor.

The interference filter used to isolate $2p\,^1P$–$3d\,^1D$ (6678 Å) light did pass the 6560 Å light from the He II $n=4$ to 6 transition. Using a monochromator, the ratio of intensities (6560 Å/6678 Å) without the filter was measured to vary from unity at 400 keV to 10 to 1 at 1100 keV. The filter cut out 96.6% of the 6560 Å light relative to its transmission at 6678 Å. The He II line was isolated using a filter centered at 6561 Å with a 10 Å bandwidth. Its polarization was measured at the same distance from the foil at which the ^1D measurements had been made. The polarization P varied smoothly between +5.5% at 500 keV and +2.8% at 900 keV for a beam-current density of 30 $\mu A/cm^2$. Current densities of 6 $\mu A/cm^2$ gave polarizations about 1.5% lower across the energy range. The $3d\,^1D$ polarization measurements were corrected accordingly. The maximum adjustment was at 900 keV, where the measured value for $A_0^{col}(0)$ of 8.5% was corrected to 12.2%. The "contaminant" effect was negligible at 400 keV. The magnitude of the correction varied smoothly between these limits at intermediate energies.

B. Secondary electron and temperature measurements

Secondary electron and temperature measurements have been described previously.[12] Data reported here were taken at Argonne for He^+ beam energies above 400 keV. The number of secondary electrons emitted from the foil per incident ion was determined by measuring the current at an aluminum plate, 2×3 cm, 2 mm from the foil and 1 cm from the beam, with its long edge parallel to the beam direction. The anode current reached a plateau for bias voltages above +500 V. The foil holders were grounded. These measurements did not distinguish electron energy or angle of emission, but should give accurate values for relative yields. Owing to the geometry of the anode, electrons emitted from the exit surface of the foil should be collected preferentially to those emitted from the entrance surface.

During the secondary electron measurements, foil temperature was monitored using an Ircon 300L bolometer.[12] The 6.1 $\mu g/cm^2$ foils used in this experiment had a measured spectral emissivity of 0.12 for emission between 2 and 2.6 μm at an angle of 39°±2° to the foil normal. The effective emissivity, accounting for attenuation in the fused silica viewing port, was 0.07. Foil temperature was measured as a function of beam-current density between 400 and 1400 keV. Results obtained using different foils were reproducible within experimental error.

III. RESULTS

A. Alignment data

The alignment data for the $n=3$ states are shown in Figs. 1–4. These results are tabulated in Ref. 17. The solid points were taken with beam-current densities of 30±5 $\mu A/cm^2$; open points were taken with 6±2 $\mu A/cm^2$. Each point repre-

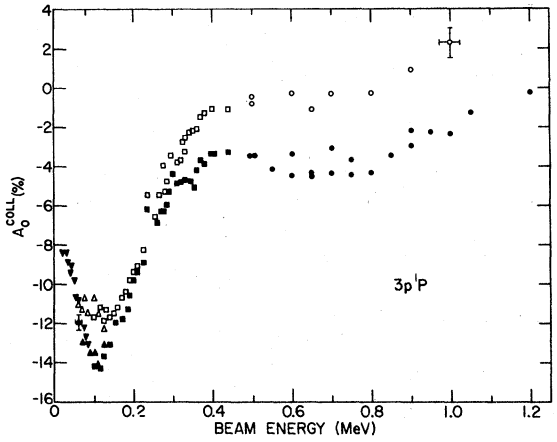

FIG. 1. A_0^{col} of the He I $3p\,^1P$ state vs beam energy after the foil. Foil areal density: 5–6.5 $\mu g/cm^2$. Open points: $j = 30 \pm 5\ \mu A/cm^2$, solid points: $j = 6 \pm 2\ \mu A/cm^2$. Data were taken at Bell Labs (Ref. 17) (upside down triangles), Chicago (triangles), Toledo (squares), Argonne (circles). Alignment error bars are statistical; the error bar at 1.0 MeV includes uncertainty due to the correction for instrumental polarization. Energy error bars represent calibration uncertainty.

sents one run taken with one foil. Typical error bars are shown in each figure. The alignment errors indicated are statistical and do not account for possible systematic variations due to uncertainty in δ or unknown foil variables. Alignment variations over the energy range appear, in general, to be statistical in nature. Nonstatistical scatter in the data may be caused by uncontrollable foil variables. We have noticed that if a foil breaks or developes pinholes more quickly than normal, polarization data taken while the foil was "good" is often anomalous. For this reason data from a run in which the foil broke were not used. Horizontal error bars represent the accuracy of the energy calibration. Data taken at different laboratories match quite well. The $3p\,^1P$ results below 500 keV have been published before.[10] Data above 500 keV complete earlier, less-detailed measurements.[11]

The current (temperature) dependence is seen to be a general phenomenon, and is somewhat more pronounced at higher energies. More detailed measurements of the current dependence for the four lines at energies of 125 and 650 keV are shown in Figs. 5 and 6. The data were fit to a straight line. The values of S_j, the line's slope,

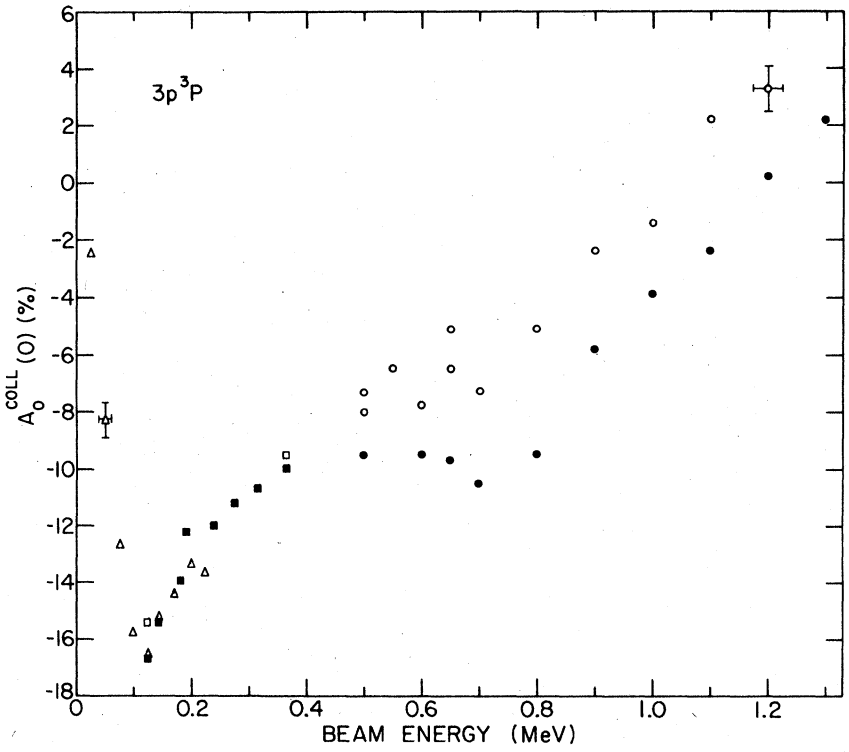

FIG. 2. A_0^{col} (0) of the He I $3p\,^3P$ state vs beam energy after the foil.

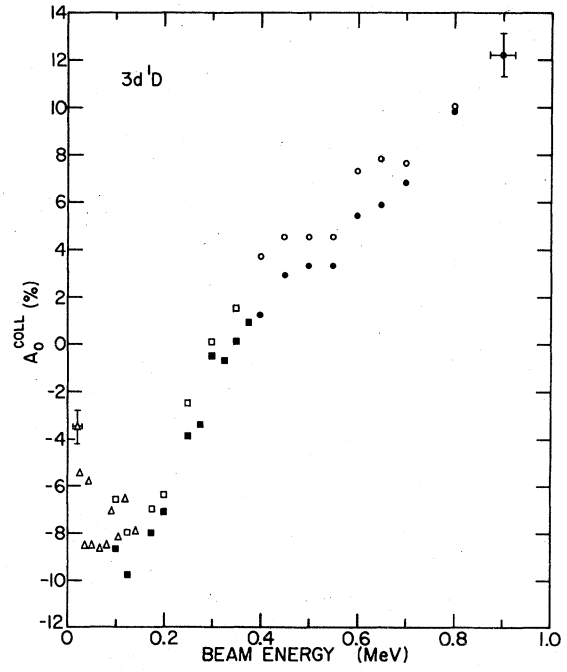

FIG. 3. A_0^{col} of the He I $3d\,^1D$ state vs beam energy after the foil. Alignment error bar at 0.9 MeV includes statistical uncertainty resulting from correction for contaminant 6560-Å transition (see text).

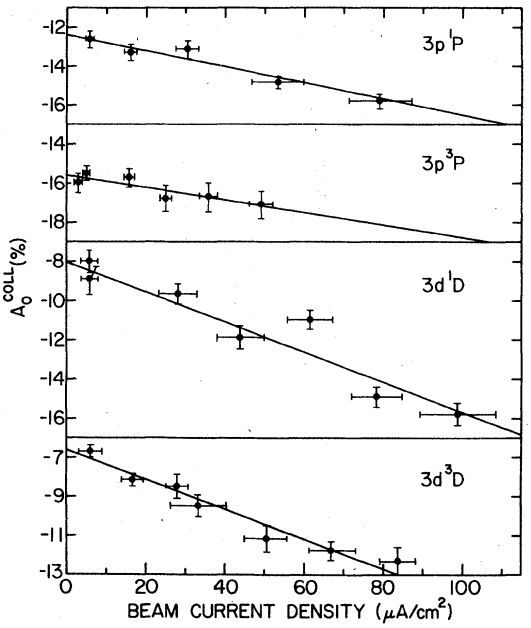

FIG. 5. A_0^{col} (0) vs beam-current density for the n = 3 He I states at 125-keV postfoil energy. Beam-current error bars correspond to beam fluctuations during the run. Slope of indicated line = S_j.

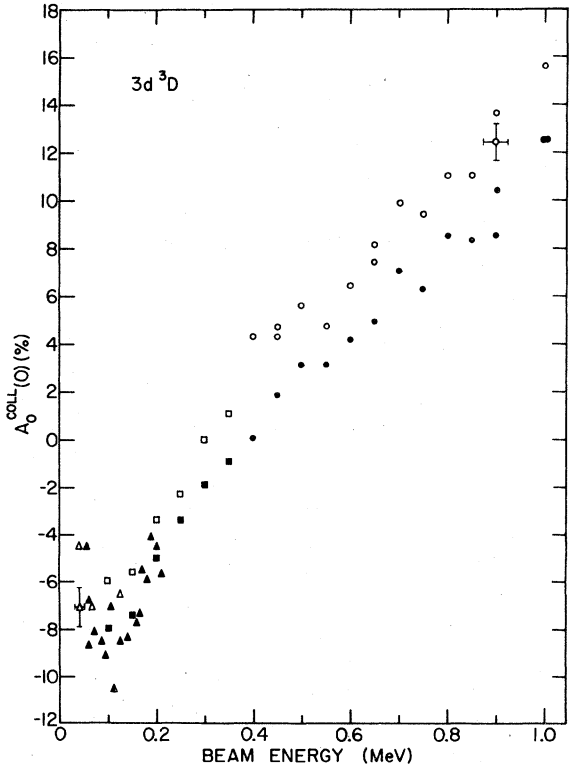

FIG. 4. A_0^{col} (0) of the He I $3d\,^3D$ state vs beam energy after the foil.

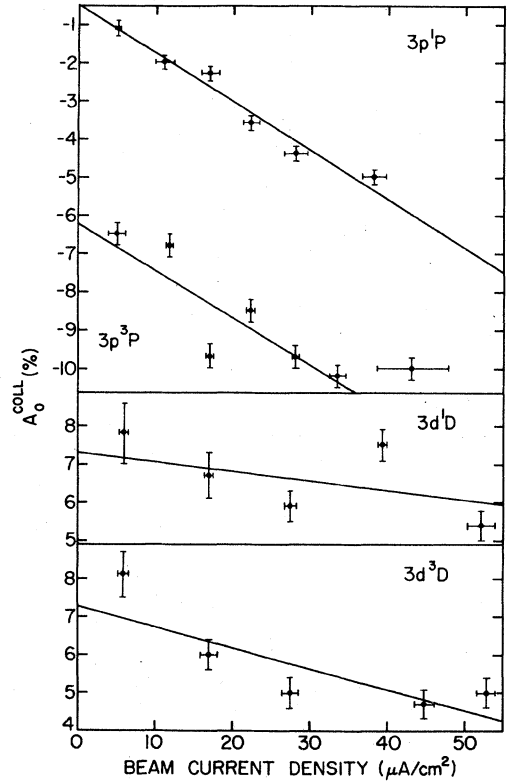

FIG. 6. A_0^{col} (0) vs beam-current density for the n = 3 He I states at 650-keV postfoil energy.

TABLE I. Beam-current density dependence of $A_0^{col}(0)$.

Energy	State	$-S_j$ (10^{-4} cm^2 μA^{-1})
125	$3p\,^1P$	4.2(1.2)
125	$3p\,^3P$	3.2(1.2)
125	$3d\,^1D$	7.7(1.4)
125	$3d\,^3D$	8.0(1.4)
650	$3p\,^1P$	12.9(1.0)
650	$3p\,^3P$	12.1(1.4)
650	$3d\,^1D$	2.3(1.6)
650	$3d\,^3D$	5.3(1.4)

are listed in Table I. Note that S_j is always negative and, to within the uncertainty of the linear fit, independent of excited-state multiplicity.

The curves resulting from a hand fit to the high-current data are shown in Fig. 7. The high-current data from Ref. 11 (30 μA/cm^2) for the $4d\,^1D$ state are also included. All states exhibit a minimum of alignment, A_0^{col}, in the vicinity of 110–120 keV except the $4d\,^1D$ state, which reaches a minimum at about 80 keV. The P states have broad secondary minima between 600 and 800 keV. All three D states exhibit a "shoulder" at 550 keV. It is most readily seen in the singlets, although it occurs in the low-current $3d\,^3D$ data as well. More detailed measurements with smaller energy increments would be necessary to unambiguously verify its existence. As the beam energy increases, all five states tend toward positive A_0^{col}. The D states cross zero between 350 and 400 keV. The P states cross at 1200 keV. At the lowest energies, A_0^{col} again increases but remains negative in all cases.

An interesting feature of this data is the spin dependence of P state alignment. Such a spin dependence for the HeI $n=3$ P states has recently been seen in tilted-foil experiments,[18] and general

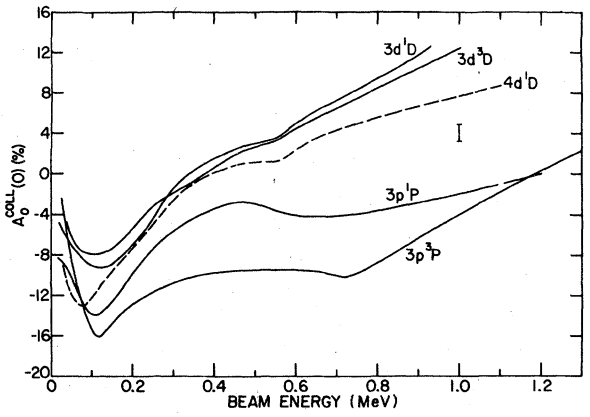

FIG. 7. A_0^{col} (0) vs beam energy after the foil for 5 HeI excited states (see text). High current data is shown. Vertical bar corresponds to typical statistical error.

spin-dependent features of the beam-foil-excitation process have been observed for some time.[19,20] While the values of alignment are different for the two P states, their energy dependent features are qualitatively similar. In contrast, the two D states have, within experimental error, identical alignment throughout the energy range studied. The $4d\,^1D$ state, while similar in overall features to the $n=3$ D states, has a generally lower alignment at all energies. Measurements of alignment for one or another of these states at isolated energies have been made at other laboratories. These results are presented in Table II. The agreement with our data is quite good, with the exception of the $3p\,^3P$ measurement at 238 keV and the 40-keV $4d\,^1D$ value.

There are several similarities between foil-excited H Ly-α data[6-9] and our results (see Fig. 3 of

TABLE II. Summary of measurements by other investigators.

Investigators	State	Energy (keV)	j(μA/cm^2)	$A_0^{col}(0)$, (%)	This work	j(μA/cm^2)
Brooks and Pinnington[a]	$4d\,^1D$	160	18	−10.0(1.0)	−9.1(0.6)	25
	$3d\,^1D$	160	18	−9.3(1.1)	−8.7(0.7)	30
	$3p\,^1P$	160	18	−13.3(0.5)	−12.2(0.5)	30
	$3p\,^3P$	160	36	−15.0	−14.4(0.8)[e]	30
Yellin *et al.*[b]	$4d\,^1D$	40	not specified	−16.7(2.5)	−12.4(0.8)	25
	$3d\,^3D$	40	not specified	−6.7(2.8)	−7.1(0.9)	6
Burns *et al.*[c]	$3p\,^3P$	200	not specified	−14.5(0.5)	−12.9(0.8)	6
Bromander *et al.*[d]	$3p\,^3P$	238	~250(?)	−8.0(1.0)	−12.9(0.7)	30

[a] Reference 21.
[b] Reference 22.
[c] References 18 and 23.
[d] Reference 24.
[e] Interpolated value.

Ref. 9). A broad dip in A_0^{col} at about 25 keV corresponds closely in velocity to the minima for He. In addition, there is a "plateau" between 70 and 150 keV similar to the features in He between 500 and 800 keV. We shall discuss these similarities shortly.

B. Secondary electron and temperature data

The ratio of anode current with the foil in place to beam current was measured as a function of beam current. To the extent that electrons emitted from the foil's entrance surface are not detected by the anode, this ratio will equal the number of secondaries emitted per incident ion from the downbeam surface of the foil. In any case, the anode current and the secondary current from the exit surface will vary proportionately with foil temperature.[25] The current ratio γ is shown as a function of foil temperature (beam current) at 800 keV in Fig. 8. Vertical error bars correspond to typical fluctuations in the anode current. The decrease of γ with increasing foil temperature is due to the enhanced density of the "phonon gas" in the foil. Inelastic collisions of secondary electrons produced in the foil bulk with phonons reduces the ability of the electrons to surmount the surface barrier and escape. Thus the decrease of secondary emission is analogous to the increase of bulk resistivity with temperature.[25] Note that γ ranges between 9 and 15 at this energy. Meckbach,[26] measuring secondary emission from carbon foils bombarded by H^+, has measured a γ of ~3 for the exit surface at 200 keV. Secondary flux at a given ion velocity should be directly proportional to the stopping power of that ion in the solid.[17,25] Thus we expect γ for He^+ at 800 keV to be about 12. The measured value for γ therefore implies we are measuring few electrons emitted from the upbeam foil surface. For a given foil temperature, γ increases with energy. This increase is also understood in terms of stopping power, although the two quantities do not vary in strict proportion. At 100 keV and a foil temperature of 600 K, we measure γ to be ~11, whereas at 800 keV, its value is about 15. Sternglass has shown that other energy-dependent quantities may effect secondary yield.[25]

Secondary electron emission appears to decrease linearly with temperature at all energies (see also Fig. 6 of Ref. 12). To give a rough quantitative measure of the temperature dependence of γ we have fitted the data at each energy with a straight line. The slopes of these lines are plotted versus energy in Fig. 9. The five low-energy points have been published previously.[12] Error bars represent the uncertainty in the least-squares fit to the data. There is a general decrease of S_γ with increasing energy. We interpret this again as being due to the increase of stopping

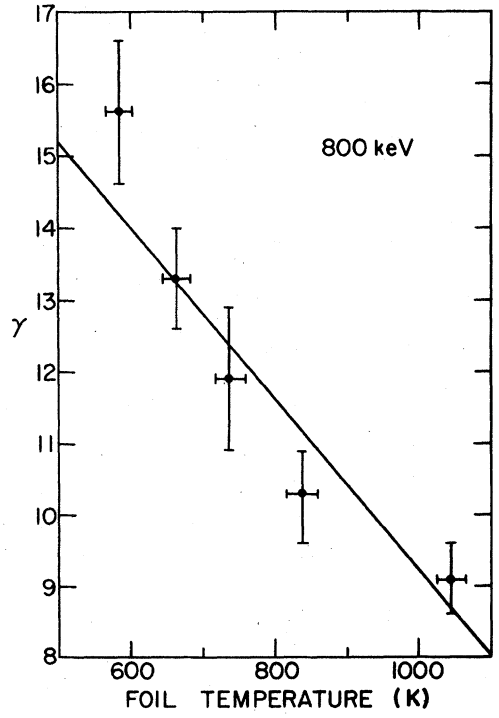

FIG. 8. Secondary electron current to beam-current ratio ($\equiv\gamma$) vs foil temperature for 800-keV He exit energy. S_γ is the slope of the fitted line. Error bars represent fluctuations of anode current.

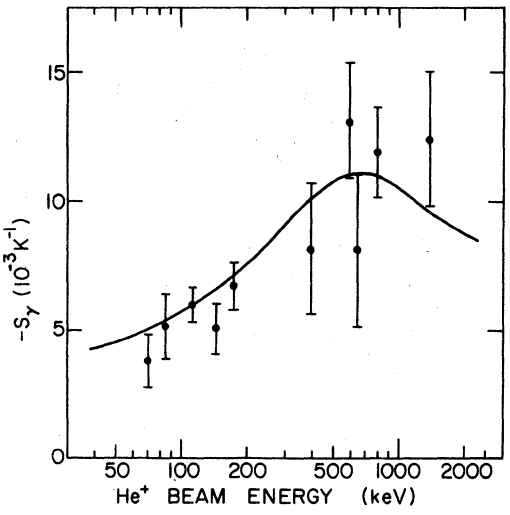

FIG. 9. S_γ vs beam energy. Total stopping power curve for He^+ on carbon is normalized at 117 keV (Refs. 12, 27, and 28). Error bars correspond to uncertainty in least-squares linear fit of γ vs foil temperature.

power. The percentage change in γ for a given change in foil temperature should be fairly independent of energy. Thus, as γ increases with stopping power, $d\gamma/dT$ should decrease accordingly. Stopping power for He^+ on carbon,[27,28] normalized to the 117-keV value of S_γ, is also shown in Fig. 9.

Foil temperature was measured as a function of beam-current density between 400 and 1400 keV. A typical result is shown in Fig. 10. The temperature error bars represent the fluctuation of thermal power from the foil during the run. They do not include error resulting from uncertainty in foil emissivity. The functional dependence of foil temperature on beam current is described well by[12]

$$J\langle dE/dx\rangle t = 2A\epsilon\sigma(T^4 - T_0^4), \tag{13}$$

where J is the beam current, t is the foil thickness, T is the foil temperature at the beam spot, T_0 is the ambient temperature, σ is the Stefan-Boltzmann constant, ϵ is the integrated emissivity of the foil, A is the area of the beam spot, and $\langle dE/dx\rangle$ is the average stopping power per unit thickness in the foil. Radiation is the principal energy loss mechanism.[12] For a given beam-current density, foil temperature was seen to vary only slightly with energy. This is because temperature depends on $\langle dE/dx\rangle^{1/4}$, which changes by only 4% in our energy range.[27]

IV. DISCUSSION

A. Energy dependence of alignment

In this section we compare our data for foil-collision-induced alignment with analogous single-collision measurements. We first discuss our results in terms of simple impulsive momentum-transfer collisions. We then compare them with

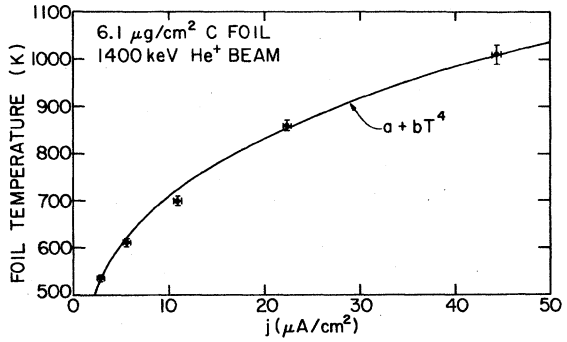

FIG. 10. Foil temperature vs beam-current density. Least-squares fit to the functional form $j = a + bT^4$ is shown. Each data point was taken with a different foil.

alignment produced in specific collisions of He with electrons, protons, and heavy atomic and molecular ions and atoms. Finally, theoretical analyses of single-collision impact-excitation data are compared with the foil results. Consequently, we can propose a preliminary binary impact model of the fast ion-foil surface interaction, modified by a longer range final-state interaction with secondary electrons.

We note that very little theoretical progress has been made even with single-collision processes in predicting relative atomic sublevel populations. Coherence parameters have been measured for only a few cases of noncylindrical geometry; for example, in electron or proton impact-excitation of H and He by coincidence measurements between the scattered projectile and the emitted photon.[29,30] Our cylindrical geometry provides some angle averaging of these processes. However, the atomic alignment and orientation parameters must be sensitive to final-state interactions which determine the shape of the wave function of the receding atom or ion. Thus the first Born approximation and its distorted-wave variants can have only limited applicability to such processes, even at high velocity.

General features of our data, however, may be understood from relatively simple considerations.[17] Assuming that production of the excited He state results from an impulsive transfer of momentum (i.e., Born approximation) between a foil atom (or group of foil atoms) and a He atom at the surface of the foil, we may write[13,31-33]

$$A_0^{\rm col}(0) = -\tfrac{1}{2}[3\langle(\hat{q}\cdot\hat{z})^2\rangle - 1], \tag{14}$$

where $\hat{q}$ is the unit vector along the momentum transfer axis and $\hat{z}$ is the beam axis. At low energy near threshold, where $\hat{q}$ must be parallel to $\hat{z}$, $A_0^{\rm col}(0) \to -1$. At high energy, as $\hat{q}$ becomes predominantly transverse, $A_0^{\rm col}(0) \to \frac{1}{2}$. Apart from the effects of resonant excitations and final-state interactions not included in such a picture, we expect a smooth variation of $A_0^{\rm col}(0)$ with energy between these two limits. Thus, the qualitative features of our data are understood quite well from these kinematic considerations.

While the general features of our data are explained by this simple-collision model, two important details are not. These are the increase of $A_0^{\rm col}(0)$ at low beam energy and the secondary minima seen clearly in the P states and as "shoulders" in the D states. We may understand the origin, if not the cause of these features by comparing our results with analogous single-collision data. We consider impact excitation of He by electrons and ions (most generally H^+) and collisions between fast He^+ and rare gases in which

the He^+ captures an electron into an excited state. We concentrate on alignment measurements of singlet states which are much more extensive and somewhat more reliable.[34]

The high-current density foil data and single-collision data for the $3p\,^1P$ and $4d\,^1D$ states are shown in Figs. 11 and 12. Most single-collision alignment results are given in the literature in terms of the observed linear polarization fraction (M/I). Thus we plot our results in this manner for the present discussion. Note that M/I is closely proportional to $-A_0^{\rm col}(0)$. The data for proton impact excitation of He (Refs. 35–38) (dashed lines) are roughly similar to ours in both cases. The proton data exhibit two maxima with the one at low energy being more pronounced. Also, M/I drops through zero and becomes increasingly negative at higher energy. In addition, M/I decreases at low energy. All these features are reflected in the foil data. We note that the foil data exhibit generally lower polarization than do the single-collision results. This is especially true in the $4d\,^1D$ case.

For electron impact excitation[39,40] we would expect M/I at threshold to be $+0.6$ and $+1.0$ for the 4922 Å and 5016 Å transitions, respectively, corresponding to $A^{\rm col}(0) = -1$. Instead, polarization decreases dramatically in this region. The cause of this dip is not well understood, but is probably related to resonant states of He^- which are known to exist near threshold.[13,41] At high energy, M/I becomes negative.

It is tempting to try to explain the secondary maxima of our beam-foil results in terms of the electron data. The slight rise in the polarization of the D states at 550 keV and of the P states between 600 and 800 keV might correspond to the onset of excitation by foil electrons. In the foil situation, the bombarding electrons are not monochromatic, but have a velocity distribution which, at least for the valence electrons, can be considered to be similar to a Fermi distribution. In the projectile frame of reference, the average electron energy is then given by

$$E = \tfrac{1}{2} m_e (v_{\rm He}^2 + \tfrac{3}{5} v_F^2) . \qquad (15)$$

The Fermi velocity in carbon is $\sim 2\times 10^8$ cm/sec. As a result, features in the beam-foil alignment curves due to electron excitation should appear at helium beam velocities of about 3×10^8 cm/sec, a value significantly lower than that which we observe for the secondary maxima. Hence this explanation seems unlikely.

Finally, the results of He^+ neutralization and excitation experiments are shown in Figs. 11 and 12.[42] The general features of these curves are independent of the target gas used. However, the degree of polarization increases with decreasing target Z. Interestingly, similar variation of M/I with Z have been seen in limited foil material dependence experiments which have been done.[43] The oscillatory structure of the polarization at low velocities is due to interference between quasimolecular levels which exist during the pickup process. Such structure is not seen in the beam-foil data. This might be due either to the lack of importance of such pickup processes or the "washing out" of oscillations by multiple

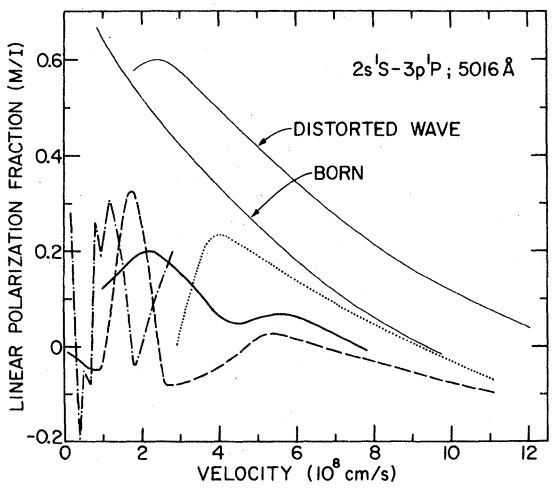

FIG. 11. Linear polarization fraction of the $2s\,^1S-3p\,^1P$ 5016 Å transition vs relative collision velocity. Heavy unbroken line represents current density (30 ± 5 μA cm^{-2}) foil data. Dashed line, proton impact excitation (Refs. 35–38); dotted line, electron excitation (Refs. 39 and 40) dashed line with dots, electron pickup by fast He^+ from Ne gas (Ref. 42). First Born and distorted wave calculations are also shown (Refs. 44 and 47).

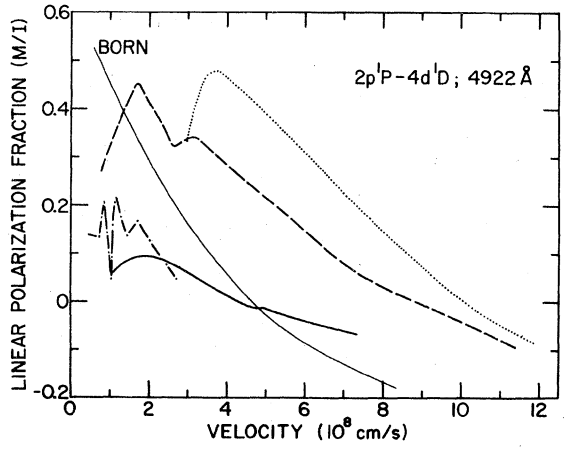

FIG. 12. Linear polarization of the $2p\,^1P-4d\,^1D$ 4922-Å transition vs relative collision velocity. Graphical designations are equivalent to Fig. 11.

collisions or electrostatic interactions at the foil surface. This "washing out" phenomenon may explain the general decrease of polarization for energies below 75 keV, where the oscillatory structure becomes increasingly pronounced in the charge-exchange data.[42]

No theories have been proposed which explain beam-foil alignment energy dependence in terms of collisional processes. Several variations of the first Born approximation[44-46] (FBA) and a distorted-wave calculation[47] treat proton impact excitation of He. The results of van den Bos's FBA calculation are shown in Figs. 11 and 12.[44] Bell's distorted-wave calculation for the $3p\,^1P$ state is shown in Fig. 11. There are some qualitative similarities between these calculations and our data. The energy dependence of alignment is relatively insensitive to the principal quantum number in the FBA, and we note little n dependence in our $n\,^1D$ results. More interestingly, the approximate energies of the zero crossings for the P and D states are predicted correctly. While these crossings occur at the same energy in the proton impact data, a large difference, predicted qualitatively in the FBA, is seen in the foil data. The distorted-wave calculation is interesting insofar as it predicts a maximum in the polarization at low energy, as observed in our data.

These results strongly suggest that the beam-foil-excitation mechanism may be comprehensively described as an impact excitation by the surface atoms, as opposed to a charge exchange or simple electron impact excitation. Proton collision data exhibit all the major features present in the foil results: A sharp increase of M/I to a first maximum at low energy followed by a smooth decrease and a second maximum at higher energy. Impact excitation of He by other projectiles[38] (H, H_2^+, H_3^+, He) yields results which are qualitatively similar to those for protons. There is virtually no projectile dependence for the $4d\,^1D$ state. For $3p\,^1P$ excitation, the secondary maximum is somewhat suppressed. Thus carbon atom-helium collisions could be reasonably expected to give similar energy-dependent results. The secondary maxima in M/I of our curves occur at the wrong energy to be explained by an electron impact model. Charge-exchange excitation data are dissimilar to the foil results. This implies that simple electron capture into an excited state is not important in the beam-foil alignment production mechanism.[48-50]

We thus propose that the final surface excitation occurs as a two-step process. A few Å below the surface, a foil electron gains correlation with the fast He^+ core ion. This transient He "atom" is subsequently excited in an impact with one or more carbon atoms in the last foil monolayer.

The P-state spin dependence remains a puzzle. Qualitative features of the data do not depend on spin, but alignment magnitudes do. Following the general assumption that spins are not aligned by the collision,[15] the only first-order difference between singlets and triplets is in their energy levels. It is perhaps significant that the singlet-triplet difference in electron correlation energy is much larger for the P than for the D states. Correlation effects in the final surface excitation process might well account for the P state variations. Ion-atom collisions of the type just discussed are highly spin dependent. Excitation probabilities and alignments of the $3p\,^3P$ state[38] excited by He^+, H_2^+, and H_3^+ collisions with He gas differ substantially from equivalent singlet data.[51] Thus while it is not understood (as it is not understood in the single-collision case), the beam-foil interaction spin dependence is not unexpected.

As mentioned earlier, H and He foil-excitation data are similar in their energy dependence. Thus, it seems likely that similar processes are also responsible for foil collision-induced alignment in hydrogen. In this regard, there is an interesting discrepancy between the H data of Winter[8,9] and that of Dobberstein *et al.*[6] Above 700 keV (1.2×10^9 cm/sec), Winter's data decrease in magnitude, reaching zero at ~1600 keV (1.8×10^9 cm/sec). The Dobberstein data show a trend toward more positive values of A_0^{∞} at high energy as expected in the simple momentum-transfer model. Thus, the high energy data of Winter seem to be unphysical, and may result from a systematic error which becomes important as counting rates decrease.

B. The model of Kupfer and Winter

The model of Kupfer and Winter (KW) represents the only attempt to date to explain the energy dependence of beam-foil collision-induced alignment.[8] Thus we briefly discuss our results in terms of this model. KW consider a hydrogen atom excited (by unspecified means) to an $n=2$ state emerging from the surface of the foil where it encounters a strong (~10^8 V/cm) electric field created by the surface dipole layer.[52,53] They then calculate in the sudden approximation the time dependence of the excited-state density matrix from which they derive the final alignment as a function of energy. No Stark mixing is assumed between the $n=2$ and higher-n levels. The model assumes that experimentally measured quantities such as relative S- and P-state production cross sections may be used as initial parameters in the density

matrix before the H atom encounters the electric field. This assumption is incorrect; any experimental measurements are *a priori* subject to the action of the postulated surface electric field. In addition, the initial parameters are given values which themselves depend strongly on energy. Thus one problem is replaced by another. The energy dependence of the initial density matrix components remains unexplained.

In the case of He, the obvious choice for the initial parameters are those obtained from a single-collision experiment. Here the final-state perturbation is through an electric field of different symmetry. We, however, note that the energy dependence of these data and the foil results are so similar that modification of the density matrix by a surface electric field becomes virtually superfluous. Consequently we have applied a similar but more restrictive model to our data. As the simplest assumption, we take both initial-state populations [$\sigma_{ii}(0)$ in the density matrix] and coherence terms [$\sigma_{ij}(0); i \neq j$] to be independent of energy. The purpose of our calculation is to determine if the energy dependence of alignment can be explained by the action of the electric field alone. It should be noted that assumptions of field uniformity over the atomic radii and of noninteraction with other n levels are even more tenuous in our case than they are for H $n=2$ states. Time dependence of the density matrix is calculated using hydrogenic wave functions with $Z=1$. The $l, m_l = 2, 2$ population is taken to be independent of time. Because we diagonalize the Hamiltonian with respect to the Stark interaction (the Stark effect is linear above $\sim 5\times 10^6$ V/cm for He I $n=3$ states), spin dependence of alignment cannot be explained with this model. Thus we consider only singlet states. In addition to the initial values of the density matrix, the alignment depends on the phase integral of the field ϕ[8]:

$$\phi \propto \bar{E}_z d/v\,, \tag{16}$$

where $\bar{E}_z$ is the average value of the surface field, d is the effective extent of the field from the foil, and v is the velocity of the atom. The alignment of the $3p\,^1P$ and $3d\,^1D$ states are plotted versus $1/v$ in Fig. 13. The ^1P data are fit in three ways. Curve A is the best fit with no initial alignment [$^P\sigma_{\pm 1}(0) = {}^P\sigma_0(0)$, etc.] of coherence [$\sigma_{ij}(0) = \alpha_{ij}\delta_{ij}$]. The independent adjustable initial density matrix parameters used to give the best fit are listed in Table III. Curve B was obtained assuming initial alignment with no coherence. Curve C is the best fit allowing nonzero coherence terms as well as initial alignment. Even curve C with seven adjustable parameters is unable to duplicate the high energy ($1/v \approx 0.4$) ^1P minimum. The values

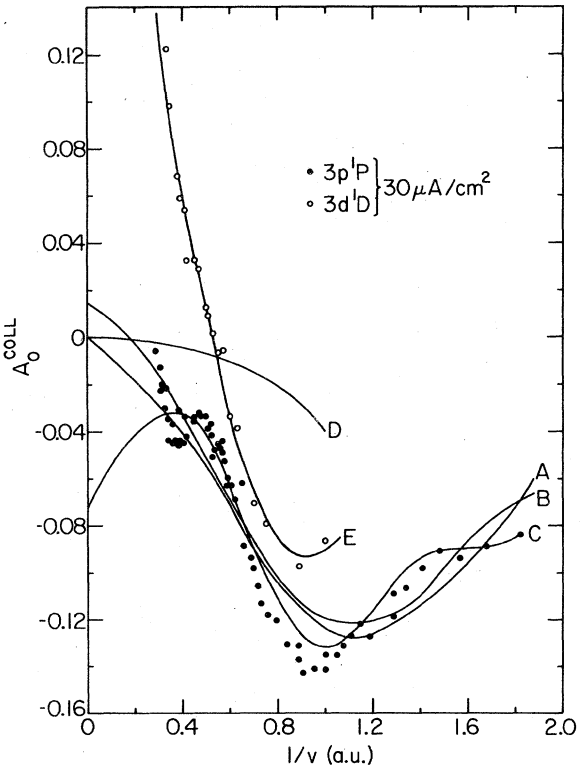

FIG. 13. A_0^{col} (0) of the $3p\,^1P$ and $3d\,^1D$ states vs $1/v$ (see text).

TABLE III. Surface field fitting parameters.

Fit	Independent initial density matrix fitting parameters ($^P\sigma_0(0) \equiv 1$)	$\bar{E}_z d$ (a.u.)	Reduced χ^2
A	$^S\sigma = 7.18$ $^P\sigma = 1.00$ $^D\sigma = 0.91$	0.025	15.1
B	$2\,^S\sigma + {}^D\sigma_0 = 3.98$ $^P\sigma_0 = 1.00$ $^P\sigma_1 = 1.04$ $^D\sigma_1 = 0.82$	0.029	13.6
C	$2\,^S\sigma + {}^D\sigma_0 + 2\sqrt{2}\,\mathrm{Re}\,{}^{SD}\sigma = 2.68$ $\sqrt{2}\,\mathrm{Im}\,{}^{SP}\sigma - \mathrm{Im}\,{}^{PD}\sigma_0 = 0.03$ $\mathrm{Im}\,{}^{PD}\sigma_1 = 0.06$ $^P\sigma_0 = 1.00$ $^P\sigma_1 = 0.80$ $^P\sigma_1 = 0.67$	0.058	10.9
E	$^S\sigma = 0.01$ $^P\sigma_0 = 1.00$ $^P\sigma_1 = 0.37$ $^D\sigma_0 = 0.35$ $^D\sigma_1 = 0.00$ $^D\sigma_2 = 0.27$	0.031	4.6

for $\bar{E}_z d$ range between 0.025 and 0.058, corresponding to a field of 10^8 V/cm extending ~1 Å from the foil. While this value is expected from calculations of the surface dipole field, these results emphasize the poor physical basis of the model. KW get the best fit to the H data with $\bar{E}_z d = 0.8$.

The fitting parameters corresponding to curve A allow us to unambiguously predict the D-state alignment energy dependence. This result is shown as curve D. Because it has increasingly positive values of $A_0^{\infty 1}$ at high energy curve B appears to give the best physical agreement with the P-state results. Thus, using the same assumptions of initial alignment with no coherence, we fit the D data. This result is shown as curve E. The initial parameters corresponding to fits E and B are considerably different. For example, the D-state fit predicts an initial P-state alignment of −0.36. Clearly such a simple surface field model does not explain our results. Indeed, the most likely effect of surface electric fields is to be one of alignment reduction. As we have seen, He alignment resulting from single collisions with ions is generally larger in magnitude than foil collision-induced alignment. On a microscopic scale, the foil surface looks like the Himalayas. Thus such surface fields would tend to reduce anisotropy in outgoing atoms. Single-collision alignment production mechanisms are, as a result, altered by solid-state factors. The temperature dependence of alignment is another example of this. In light of the similarity between single-collision impact excitation and foil data, we conclude that surface fields are not required to explain the energy dependence of beam-foil collision-induced alignment.

C. Temperature dependence of alignment

We have shown previously that the variation of alignment with beam-current density results from heating of the foil by the beam.[12] Such temperature changes affect several foil properties. The distribution of electrons in the foil is altered. The Fermi temperature of carbon, however, is 78000 K. Thus an increase of 500 K in the foil temperature affeots this distribution negligibly. The normally amorphous structure of carbon foils graphitizes at about 800 K resulting in a considerably different value for the electrical conductivity.[4,54,55] These changes are irreversible, however, indicating that they cannot explain our results, which are independent of the thermal history of the foil. Finally, our data are independent of chamber pressure between 2×10^{-7} and 2×10^{-5} Torr. Thus temperature dependence of surface contamination must also be ruled out as an explanation.

The remaining possibility is that secondary electrons created by the ion core in the foil bulk influence the excited-state production at the surface. There are two pieces of circumstantial evidence to support this conclusion. First, the fractional change of γ is large over the temperature range of these experiments. Electrostatic interactions between the emerging atom and the secondary electrons are certainly strong. A good estimate for the maximum depth at which secondaries can be produced and still escape the surface is 15–20 Å.[17,25] First-order secondaries created in distant collisions between ions or δ rays and carbon electrons will have energies of ~25 eV initially. Thus they may undergo no more than 2 or 3 inelastic collisions with target atoms before they lose their ability to surmount the surface potential barrier.[56] To a good approximation, we may assume that these electrons are scattered isotropically by the carbon atoms.[57] As a result, an electron which is not scattered consistently towards the surface will not escape. It is therefore reasonable to expect that a great majority of the secondary electrons will emerge within 20 Å of the ion's track. Thus the electronic environment experienced by the He atom as it leaves the surface depends strongly on foil temperature.

Secondly, there is a general correlation between S_J and S_γ; at high energy, where γ is more sensitive to foil temperature, the current temperature dependence of alignment is more pronounced. This does not hold strictly at all energies. There appears to be a dip in S_J near 250 keV for all four states. This is most evident in the $3p\,^1P$ data (see Fig. 2, Ref. 10) and is a puzzling feature we do not understand. The increase of S_γ with stopping power, however, is accompanied by an overall increase in S_J from low to high energy.

The distribution of the secondary electrons about the atom as it emerges from the foil is unclear. Heating the foil reduces the number of electrons which escape the foil, but should not substantially affect their spatial distribution. Owing to δ-ray production, some slow secondaries will precede the ion.[12,17,25] These will be produced nearer the surface, on the average, than secondaries created by glancing collisions between valence electrons and the ion, and will consequently have somewhat higher energy upon escape. Electrons emerging after the atom should do so with a time delay roughly proportional to their distance from its track. The majority of secondaries have energies of the order of 3–4 eV as they leave the surface.[26] In general, their velocity vectors are not parallel to that of the atom. Thus electron-atom interactions will be quite brief.

The increased secondary electron emission from the foil appears to enhance population of states with higher absolute values of m_l. We have shown previously that the secondary electrons are not being captured by He^+ ions.[12] Thus the mechanism whereby atomic alignment is affected by variations in the secondary flux remains obscure. One speculative possibility is shown in Fig. 14. Using our qualitative picture of the electron distribution, we consider its effect upon a P state emerging from the foil. Let us assume that by virtue of its collision with a foil atom, the He atom which exists just below the surface is excited to the $3p$ state with no initial alignment (as is the case at ~1200 keV). In (a), the atom emerges from the foil with a few secondaries surrounding the nucleus. The secondary cloud interacts most strongly with the $m_l=0$ lobes. A bit later (b), the He begins to pull away from the secondaries. Owing to electron-electron collisions, the population of the $m_l=0$ state is diminished. Finally, when the influence of the secondary electron cloud is negligible (c), the He relaxes to a state with net positive alignment. By decreasing the density of the secondary electron cloud by 30% as we do in heating the foil from 600 to 1000 K, we decrease the alignment of the $3p\,^3P$ state at 1200 keV (see Fig. 2) from 3% to zero. This corresponds to a 1% change in the relative populations of the m_l states. Thus we see that the effect of the secondaries is a relatively small perturbation on the excited state.

The experiments we have discussed provide strong circumstantial evidence that slow secondary electrons affect the alignment of the beam-foil excited states. However, it would be useful to "decouple" any effects due uniquely to foil temperature from those caused by interaction with electrons at the surface. This is difficult to do experimentally because kinetic electron emission depends only weakly on foil material and surface conditions.[25,58] Recently we attempted to learn more about electrostatic interactions between helium atoms and close charged particles at the foil surface by bombarding the carbon foils with HeH^+ molecular ions.[17,59] By varying the foil thickness the average emergent He-H internuclear separation could be controlled. While the respective distributions of protons and secondary electrons about the He atom are considerably different, the HeH^+ results have demonstrated that close, correlated charged particles can affect the alignment of emergent He excited states. He^+ experiments at low energy (<10 keV), where kinetic secondary emission is negligible, would add greatly to our understanding of these interactions.

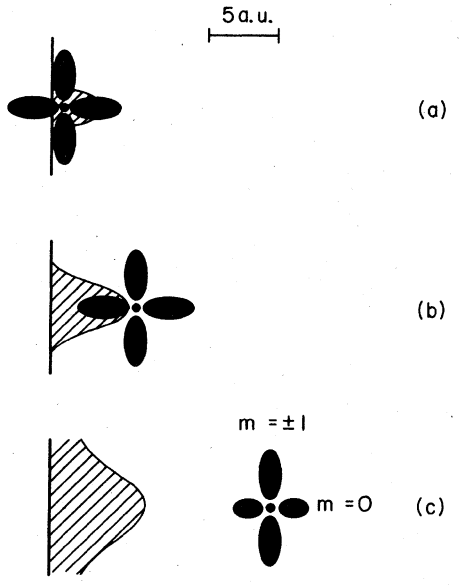

FIG. 14. Schematic diagram of the effect of secondary electron emission on atomic P-state alignment (see text).

V. SUMMARY

We have shown that the beam-foil collision-induced alignment may be understood as an atom-target ion impact-excitation process modified by solid-state effects. Our results for the energy dependence of alignment are qualitatively similar in all respects to proton impact excitation of neutral ground-state helium. The lack of strong projectile dependence in the single-collision data implies that carbon ion and atom impact excitation of neutral helium could be expected to yield similar results. Thus a simple picture of the excitation process emerges. A few Å below the final surface a He atom is formed, consisting of the doubly charged nucleus and two fast correlated electrons. As this neutral complex traverses the last monolayer of the foil, it is collisionally excited. This basic excitation process is modified by two further interactions. The net dipole field of the irregular surface reduces the collision-induced alignment. Finally, the secondary electron cloud enhances the relative population of states with higher $|m_l|$. Future theoretical treatments of the beam-foil interaction should deal primarily with these physical processes.

ACKNOWLEDGMENTS

We thank Salvador Tejero at the University of Chicago and Jim Ray, Ron Amrein, Bob Aeschlimann, Lee Hitzke, Bozydar Orszula, Art Ruthenberg, Jim Stadelmann, and Jim Timm at Argonne for their technical assistance. We also thank R.

L. Brooks for several helpful discussions. Professor J. A. Simpson kindly provided access to the University of Chicago's LASR accelerator. This work was supported by the U.S. Department of Energy, Division of Basic Energy Sciences, and grants from the NSF and the Research Corporation. One of us (T.J.G.) was given financial support in the form of an Argonne Universities Association Graduate Fellowship.

---

*Also at Ryerson Physical Laboratory, The University of Chicago, Chicago, Ill. 60637.

†This paper is submitted in partial fulfullment of the requirements for the Doctor of Philosophy degree, Department of Physics, Divison of the Physical Sciences, University of Chicago.

‡Present address: J. W. Gibbs Laboratory, Yale University, New Haven, Conn. 06520.

§Permanent address: Institut de Physique Nucleaire, Sart-Tilman B-4000, Liege, Belgium.

||Permanent address: Thin Film Division, P.O. Box 74, Dale Electronics, Norfolk, Nebraska 68701.

[1]J. H. Macek, Phys. Rev. A 1, 618 (1970).

[2]H. J. Andrä, Phys. Rev. Lett. 25, 325 (1970).

[3]H. G. Berry, L. J. Curtis, D. G. Ellis, and R. M. Schectman, Phys. Rev. Lett. 32, 751 (1974).

[4]J. Kakinoki, K. Katada, T. Hanawa, and T. Ino, Acta Crystallogr. 13, 171 (1960).

[5]M. C. Cross, Phys. Rev. B 15, 602 (1977).

[6]P. Dobberstein, H. J. Andrä, W. Wittmann, and H. H. Bukow, Z. Phys. 257, 272 (1972).

[7]H. Winter and H. H. Bukow, Z. Phys. A 277, 27 (1976).

[8]E. Kupfer and H. Winter, Z. Phys. A 285, 3 (1978).

[9]H. Winter, J. Phys. 40, C1-307 (1979).

[10]R. D. Hight, R. M. Schectman, H. G. Berry, G. Gabrielse, and T. Gay, Phys. Rev. A 16, 1805 (1977).

[11]R. M. Schectman, R. D. Hight, S. T. Chen, L. J. Curtis, H. G. Berry, T. J. Gay, and R. De Serio, Phys. Rev. A 22, 1591 (1980).

[12]T. J. Gay and H. G. Berry, Phys. Rev. A 19, 952 (1979).

[13]U. Fano and J. Macek, Rev. Mod. Phys. 45, 553 (1973).

[14]D. G. Ellis, J. Opt. Soc. Am. 63, 1232 (1973).

[15]D. G. Ellis, J. Phys. B 10, 2301 (1977).

[16]H. G. Berry, G. Gabrielse, and A. E. Livingston, Appl. Opt. 16, 3200 (1977).

[17]T. J. Gay, Ph.D. thesis, University of Chicago, 1980 (unpublished).

[18]D. J. Burns, R. D. Hight, and C. H. Greene, Phys. Rev. A 20, 404 (1979).

[19]W. S. Bickel, K. Jenson, C. S. Newton, and E. Veje, Nucl. Instrum. Methods 90, 309 (1970).

[20]H. H. Bukow, H. V. Buttlar, G. Heine, and M. Reinke, in *Beam Foil Spectroscopy*, Vol. I, edited by I. A. Sellin and D. J. Pegg (Plenum, New York, 1976).

[21]R. L. Brooks and E. H. Pinnington, Phys. Rev. A 18, 1454 (1978); R. L. Brooks, Ph.D. thesis, University of Alberta, Canada, 1979 (unpublished).

[22]J. Yellin, T. Hadeishi, and M. C. Michel, Phys. Rev. Lett. 30, 1286 (1973).

[23]D. J. Burns and W. H. Hancock, J. Opt. Soc. Am. 63, 1473 (1973).

[24]J. Bromander, L. Liljeby, and I. A. Sellin, Z. Phys. A 283, 299 (1977).

[25]E. J. Sternglass, Phys. Rev. 108, 1 (1957).

[26]W. Meckbach, in *Beam Foil Spectroscopy*, Vol. II, edited by I. A. Sellin and D. J. Pegg (Plenum, New York, 1976).

[27]S. Matteson, E. K. L. Chau, and D. Powers, Phys. Rev. A 14, 169 (1976).

[28]L. C. Northcliffe and R. F. Schilling, Nucl. Data Tables A 7, 233 (1970).

[29]See, e.g., J. Slevin, H. Q. Porter, M. Eminyan, A. DeFrance, and G. Vassilev, J. Phys. B 13, L23 (1980), and S. T. Hood, E. Weigold, and A. J. Dixon, *ibid.* 12, 631 (1979).

[30]R. Krotkov and J. Stone, Phys. Rev. A 22, 473 (1980).

[31]I. C. Percival and M. J. Seaton, Philos. Trans. R. Soc. London Ser. A 251, 113 (1971).

[32]M. Inokuti, Rev. Mod. Phys. 43, 297 (1971).

[33]J. R. Oppenheimer, Z. Phys. 43, 27 (1927).

[34]E. W. Thomas, *Excitation in Heavy Particle Collisions* (Wiley-Interscience, New York, 1972).

[35]F. J. deHeer and J. van den Bos, Physica (Utrecht) 31, 365 (1965).

[36]J. van den Bos, G. J. Winter, and F. J. deHeer, Physica (Utrecht) 40, 357 (1968).

[37]A. Scharmann and K.-H. Schartner, Z. Phys. 219, 55 (1969).

[38]D. Hasselkamp, A. Scharmann, and K.-H. Schartner, J. Phys. B 11, 1975 (1978).

[39]R. H. McFarland and E. A. Soltysik, Phys. Rev. 127, 2090 (1962).

[40]R. H. McFarland, Phys. Rev. 133A, 986 (1964).

[41]D. W. O. Heddle, R. G. W. Keesing, and R. D. Watkins, Proc. R. Soc. London Ser. A 337, 443 (1974).

[42]L. Wolterbeek Muller and F. J. deHeer, Physica (Utrecht) 48, 345 (1970).

[43]H. G. Berry, G. Gabrielse, T. Gay, and A. E. Livingston, Phys. Scr. 16, 99 (1977).

[44]J. van den Bos, Physica (Utrecht) 44, 143 (1969).

[45]L. Vriens and A. Carriére. Physica (Utrecht) 49, 517 (1970).

[46]D. Baye and P.-H. Heenen, J. Phys. B 6, 1255 (1973).

[47]R. J. Bell, Proc. Phys. Soc. London 78, 903 (1961).

[48]B. A. Trubnikov and Y. N. Yavlinski, Zh. Eksp. Teor. Fiz. 52, 1638 (1967) [Sov. Phys.—JETP 25, 1089 (1967)].

[49]A. Denis and J. Désesquelles, J. Phys. 40, 437 (1979).

[50]J. Burgdörfer, H. Gabriel, and H. Schröder, Z. Phys. A 295, 7 (1980).

[51]Single-collision triplet results have been reported in Refs. 33, 36, 37, and 40 and several other works (for a review of work before 1971 see Ref. 29). The authors of Ref. 3 feel that their triplet results may be affected by systematic error.

[52]J. Bardeen, Phys. Rev. 49, 653 (1936).

[53]J. Harris and R. O. Jones, J. Phys. C 6, 3585 (1973).

[54]J. Kakinoki, K. Katada, and T. Hanawa, Acta Cryst-

allogr. 13, 448 (1960).
[55]D. S. Kupperman, C. K. Chau, and H. Weinstock, Carbon 11, 171 (1973).
[56]L. Marton, L. B. Leder, and H. Mendlowitz, in *Advances in Electronics and Modern Physics* (Academic, New York, 1955), Vol. VII, p. 183.
[57]H. S. W. Massey and E. H. S. Burhop, *Electronic and Ionic Impact Phenomena* (Oxford, New York, 1952), Chap. II, Sec. 7.3.
[58]R. A. Baragiola, E. V. Alonso, and A. Oliva Florio, Phys. Rev. D 19, 121 (1979).
[59]T. J. Gay and H. G. Berry, J. Phys. B 13, L199 (1980).